Facies (2005) 51: 217–232
DOI 10.1007/s10347-005-0070-9

ORIGINAL ARTICLE

Michael W. Rasser · Christian Scheibner ·
Maria Mutti

A paleoenvironmental standard section for Early Ilerdian tropical carbonate factories (Corbieres, France; Pyrenees, Spain)

Received: 31 January 2005 / Accepted: 24 March 2005 / Published online: 26 May 2005

Abstract Early Ilerdian (Early Eocene, Shallow Benthic Zones 5 and 6) carbonate systems of the Pyrenees shelf were deposited after a time of severe climatic ('Paleocene–Eocene Thermal Maximum, PETM') and phylogenetic ('Larger Foraminifer Turnover') changes. They reflect the radiation of nummulitid, alveolinid, and orbitolitid larger foraminifera after remarkable biotic changes at the end of the Paleocene, and announce their subsequent flourishing in the Middle Eocene.

A paleoenvironmental model for tropical carbonate environments of this particular time interval is provided herein. During the Early Ilerdian, the inner and middle ramp deposits from Minerve, Campo and Serraduy revealed the end-member of a tropical carbonate factory with carbonate production dominated by the end-members of biotically (photo-autotrophic skeletal) controlled and biotically induced carbonate precipitation. Inner platform environments are dominated by alveolinids and in part by orbitolitids, middle platform environments are dominated by nummulitids. Corals are present, but they do not form reefs, which is a typical feature for the Eocene. Nummulite shoal complexes, which are well-known from the Middle Eocene are also absent during the studied Early Ilerdian interval, which may reflect the early evolutionary stage of this group.

M. W. Rasser (✉) · C. Scheibner · M. Mutti
Institut für Geowissenschaften, Universität Potsdam,
Karl-Liebknecht-Street 24/25,
D-14476 Golm, Germany
e-mail: rasser.smns@naturkundemuseum-bw.de
Tel.: +49-711-8936-143
Fax: +49-711-8936-100

Present address:
M. W. Rasser
Staatliches Museum für Naturkunde,
Rosenstein 1,
D-70191 Stuttgart, Germany

C. Scheibner
Universität Bremen,
FB 5,
P.O. Box 330440, D-28334 Bremen, Germany

Keywords Carbonate factory · Larger foraminifera · Ilerdian · Early Eocene · Pyrenees · Paleocene–Eocene Thermal Maximum (PETM)

Introduction

The Paleogene was the warmest time during the Cenozoic, and recorded several significant climatic events at different temporal scales. These events can be tracked by amplitude variations of the $\delta^{18}O$ deep-sea record (see Zachos et al. 2001). The most pronounced warming trend in the Cenozoic (Zachos et al. 2001), as expressed by a 1.5‰ decrease in $\delta^{18}O$, occurred from the mid-Paleocene (59 Ma) to the Early Eocene (52 Ma), and peaked with the Early Eocene Climatic Optimum (EECO, 52–50 Ma). In the latest Paleocene (55.5 Ma), a>1‰ negative oxygen isotope excursion suggests a rise of deep-sea temperature by 5–6°C in less than 10 ka, with a gradual return taking approximately 200 ka (Norris and Roehl 1999; Roehl et al. 2000). This event is termed the Paleocene–Eocene Thermal Maximum (PETM; also known as Late Paleocene Thermal Maximum, or Initial Eocene Thermal Maximum: Wing et al. 2003), and has major consequences for the biosphere. A major, short-term perturbation of the carbon cycle is recorded by a negative $\delta^{13}C$ excursion of approximately −3‰, which occurs over 10^4 years and is followed by a return to near initial values in a roughly exponential pattern over 200 kyr (Kennett and Stott 1991). This excursion affects the marine, atmospheric and terrestrial carbon reservoirs. This event is interpreted to reflect the massive dissociation of oceanic methane hydrates during the Paleocene-Eocene Thermal Maximum (Dickens et al. 1997). Following these events, the Eocene is characterized by a 17 my-long cooling trend, expressed by a 3‰ increase in $\delta^{18}O$, which culminated in the Early Oligocene in glaciation on Antarctica (Oi-1 glaciation; Miller et al. 1987). In contrast to open-water and terrestrial ecosystems, very few reports about changes in the shallow-water ecosystems spanning the Paleocene/Eocene boundary interval exist. Recent studies on

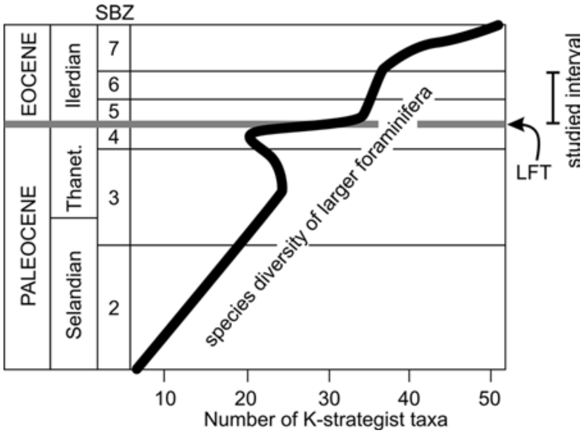

Fig. 1 Larger Foraminiferal Turnover (LFT), development of species diversity, and stratigraphic range of the studied material. SBZ: Shallow Benthic Zones of Serra-Kiel et al. (1998). Redrawn from Scheibner et al. (in press), species diversity after Hottinger (1998)

the Campo section and other platform-to-basin sections in Spain (Orue-Etxebarria et al. 2001; Pujalte et al. 2003) and Egypt (Scheibner et al. in press) proposed the synchroneity of the Larger Foraminiferal Turnover (LFT; Fig. 1), an important step in Paleogene larger foraminiferal evolution, with the PETM. The causes for the Paleogene evolution of larger foraminifera are not exclusively related to the events that occurred during the short-term PETM interval but must be also seen in the context of long-term processes. The combination of warm sea-surface temperatures that led to the demise of corals in the tropic regions, the reorganisation of the larger foraminifera after the Cretaceous-Palaeogene crisis, and changing trophic regimes, favored the dominance and diversification of larger foraminifera in the Early Eocene (Scheibner et al. in press).

During the Early Ilerdian, an extreme species radiation took place among larger foraminifera with an almost doubling of the number of K-strategists (Fig. 1) during the transition from Shallow Benthic Zone SBZ 4 (top of Thanetian) to SBZ 5 (base of Ilerdian; Hottinger 1998; Scheibner et al. in press). Two of the main larger foraminiferal groups particularly reflecting these changes are alveolinids and nummulitids. One of the best known areas of Early Ilerdian alveolinid and nummulitid limestones are the Pyrenees mountains (e.g., Hottinger 1960). They comprise several important Paleogene type localities in Spain (e.g., Campo: parastratotype of Ilerdian and Cuisian stages, lithostratigraphic type section, biostratigraphic reference section; Serraduy: lithostratigraphic type section, biostratigraphic reference section) and France (e.g., Minerve: biostratigraphic reference section, taxonomic type section; Fig. 2).

Within this Paleocene/Eocene time of global changes, the Early Ilerdian represents a particular interval. It is important to understand how the climatic and phylogenetic events impacted biogenic facies assemblages in shallow-water carbonate environments of this specific time interval with respect to the previous and successive time intervals. This study aims to present a standard section and model for paleoenvironmental interpretations of the carbonate factories (defined as places and processes of carbonate production) of Early Ilerdian carbonate systems, reflecting a time of severe global changes, and to expand former models (e.g., Hottinger 1983; Luterbacher 1984; Pautal 1987).

We studied the microfacies and paleoenvironments of Ilerdian parts of the above mentioned sections, mostly comprising Shallow Benthic Zones SBZ 5 and SBZ 6 (Early Ilerdian). As the standard section we used Minerve, which reveals the highest facies variability during this interval and from which we present a high-resolution paleoenvironmental interpretation. Campo and Serraduy serve as reference sections used for evaluation of our data and from which, therefore, lesser detailed facies data were obtained. After a literature overview of the three sections in question, we present a detailed description and palecological interpretations of the microfacies types in Minerve, followed by overviews of Campo and Serraduy (Fig. 2). The discussion part focuses on the paleoenvironmental evidence obtained from the studied larger foraminifera, the interpretation of carbonate shelf geometries, and the carbonate factories observed. Finally, a synthesis for the development of carbonate factories of an Early Ilerdian carbonate ramp is presented.

Study area and geological frame

Paleogene carbonates sediments of the North Iberian shelf form a body of relatively uniform thickness (100–150 m) tens of kilometer wide and hundreds of kilometer long (Pujalte et al. 1993). These carbonate systems comprise distally steepened ramp geometries and were deposited in an east–west elongated gulf, opening westwards into the Bay of Biscay, and surrounded by carbonate platforms to the south, east, and west (Fig. 2). Beside spatial facies patterns along the ramp, one main feature is a distinct facies change through time, with red algal and coral-dominated sediments in the Thanetian and larger foraminifera limestones in the Ilerdian (e.g., Tambareau 1994; Pujalte et al. 2003).

The development of the Pyrenees was summarized by Tambareau et al. (1994). The Paleocene is characterized by main transgressions and small-scaled sea-level fluctuations inducing a variety of terrestrial and shallow-marine successions. At the end of the Thanetian, a main tectonic event caused a widespread marine regression. A large and complex transgression followed in the Ilerdian and induced the formation of wide carbonate platforms (Fig. 2), which are the subject of the current study. At the end of the Early Ilerdian (not included in the current study), the transgression reached the surroundings of the Montagne Noir and caused deposition of marls over the former carbonate platforms. The studied carbonate successions from France (Minerve) and Spain (Campo, Serraduy) were deposited on the more eastern part of this foreland. As shown in Fig. 2, they comprise different proximities with respect to the former coastline.

Minerve is a reference section for the Shallow Benthic Zone SBZ 5 (Serra-Kiel et al. 1998) and the locus typicus of *Alveolina minervensis*. This SBZ corresponds

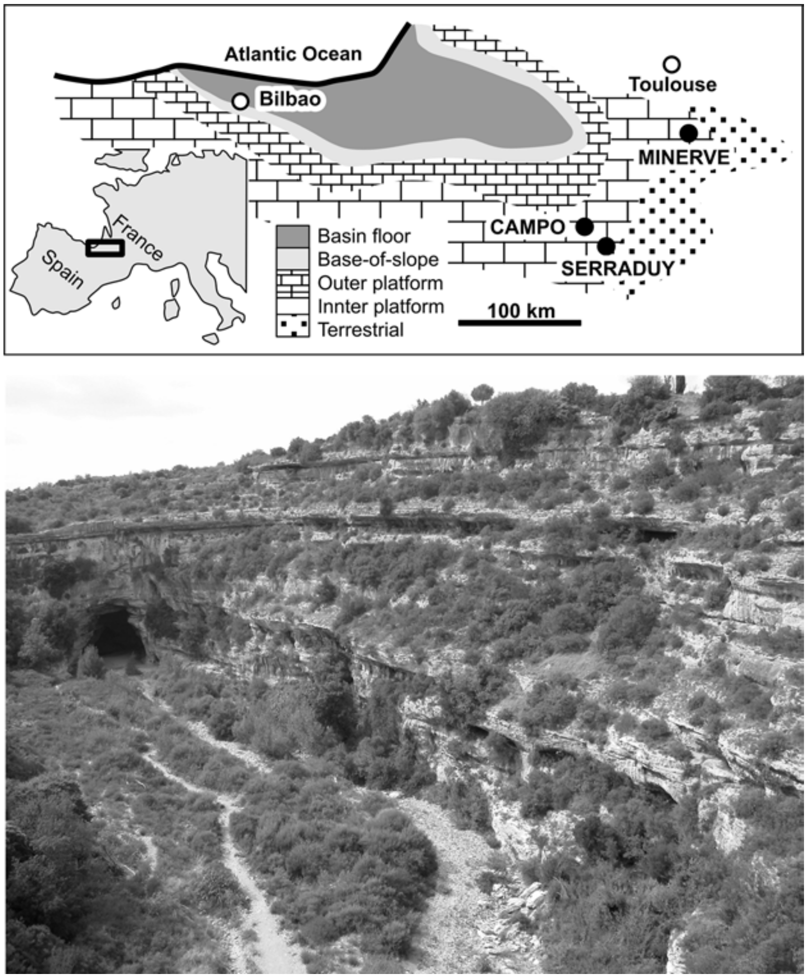

Fig. 2 Above: study area, showing the platform carbonates of the Pyrenean area during the Late Paleocene–Early Eocene. Note the position of studied section relative to the terrestrial hinterland to the east. Redrawn from Pujalte et al. (2003). Below: outcrop photograph of the complete Minerve section (ca. 55 m thick), close to the town Minerve (France)

with 'Early Ilerdian 1' of Hottinger and Schaub (1960), which represents the earliest Ilerdian zone. Hottinger (1960) reports *Alveolina ellipsoidalis, A. pasticillata, A. minervensis, A. moussoulensis, A. subpyrenaica,* and *Glomalveolina lepidula* from this section, suggesting that it represents a time span from SBZ 5 to SBZ 7.

Campo is the paratype section for the Ilerdian and Cuisian (Schaub 1969, 1992) and the lithostratigraphic type section of the Navarri Formation (overview in Robador 1991). It is also a reference section for SBZ 1, SBZ 3, SBZ 4, SBZ 5 (Early Ilerdian 1), SBZ 6 (Early Ilerdian 2), SBZ 7, SBZ 8, SBZ 10, SBZ 11 and SBZ 12 (Serra-Kiel et al. 1998). Hottinger (1960) reports Late Paleocene *Glomalveolina primaeva, Fallotella alavensis* and Eocene *Alveolina avellana, A. dolioliformis, A. varians, A. globula,* and *Glomalveolina pilula* from this section, which suggests a time span from SBZ 3 to SBZ 6. Robador (1991) noted that the top of SBZ 4 is marked by a karstified horizon with *Microcodium* sp., followed by 7 m of terrestrial sediments, above which the Ilerdian limestones with alveolinids commence. Within this terrestrial interval, Schmitz and Pujalte (2003) noticed a δ^{13}C excursion (CIE), which they postulated as the Paleocene–Eocene boundary. Molina et al. (2003) suggested on the basis of a more continuous, but low-resolution δ^{13}C record a position approximately 10 m higher for the boundary. Calcareous nannofossils were studied amongst other by Kapellos and Schaub (1973) and Orue-Etxebarria et al. (2001). Larger Foraminifera were investigated in detail by Hottinger (1960), Schaub (1966, 1969) and Kapellos and Schaub (1975). Eichenseer and Luterbacher (1992) reported differences in Ilerdian subsidence rates. While the subsidence rates remained stable in the Tremp section, they increased from the Middle Ilerdian in Campo. This increased subsidence, which would bring the carbonate environment away from the photic zone, is seen as the cause for the disappearance of alveolinids and appearance of the nummulitids upsection.

Serraduy represents a reference section for the SBZ 5 (Early Ilerdian 1) and SBZ 6 (Early Ilerdian 2; Serra-Kiel et al. 1998) and is the lithostratigraphic type section for the Serraduy Formation (overview in Robador et al. 1991).

Results and facies interpretations

Minerve section

The measured section (Fig. 3) spans 55 m, and comprises shallow-water carbonates, mixed with siliciclastics in the

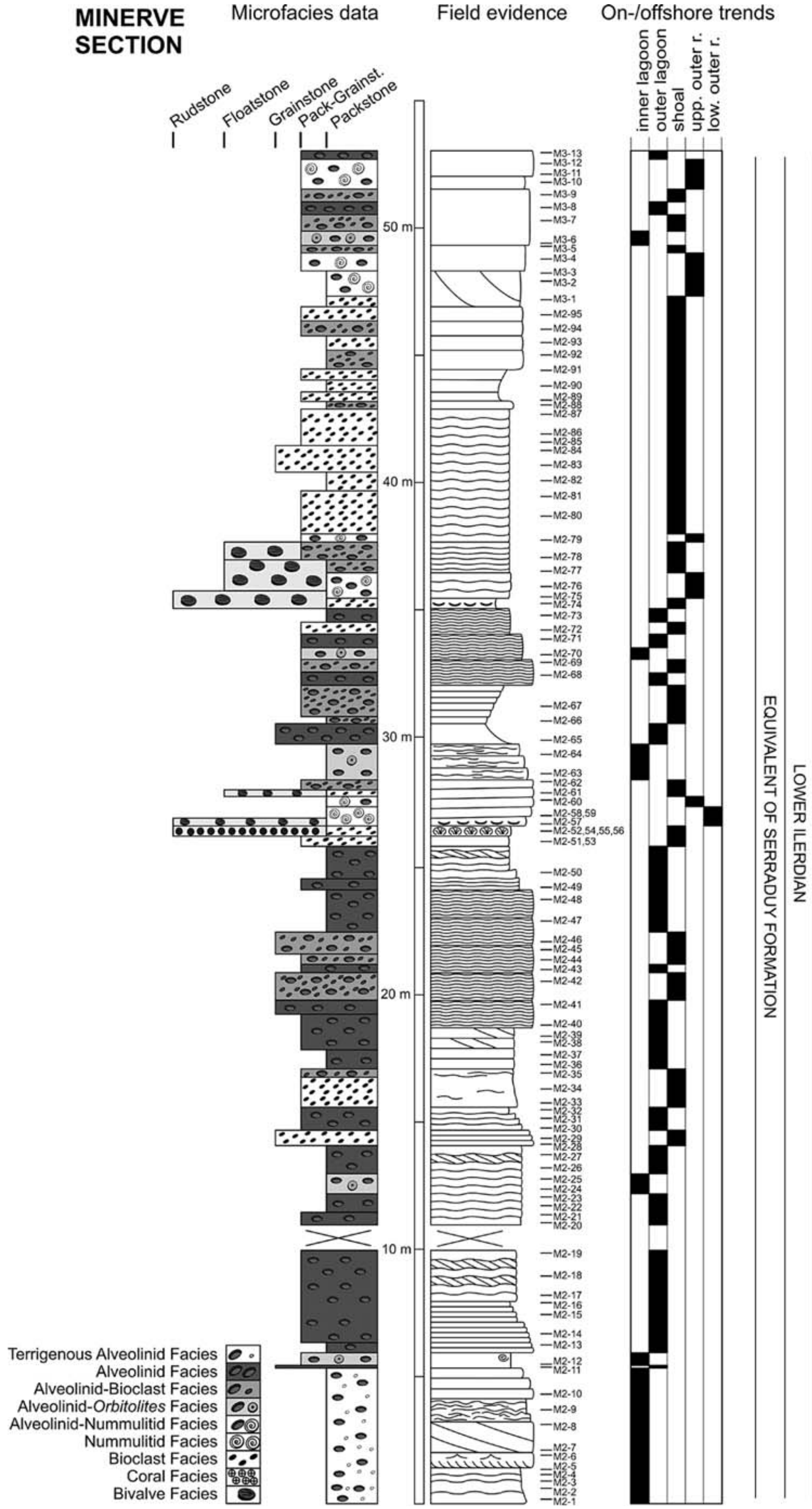

Fig. 3 Minerve section, showing facies types on the left (wideness of columns depend on facies type), weathering profile revealed from field measurements, and onshore/offshore trends revealed from paleoenvironmental facies interpretation

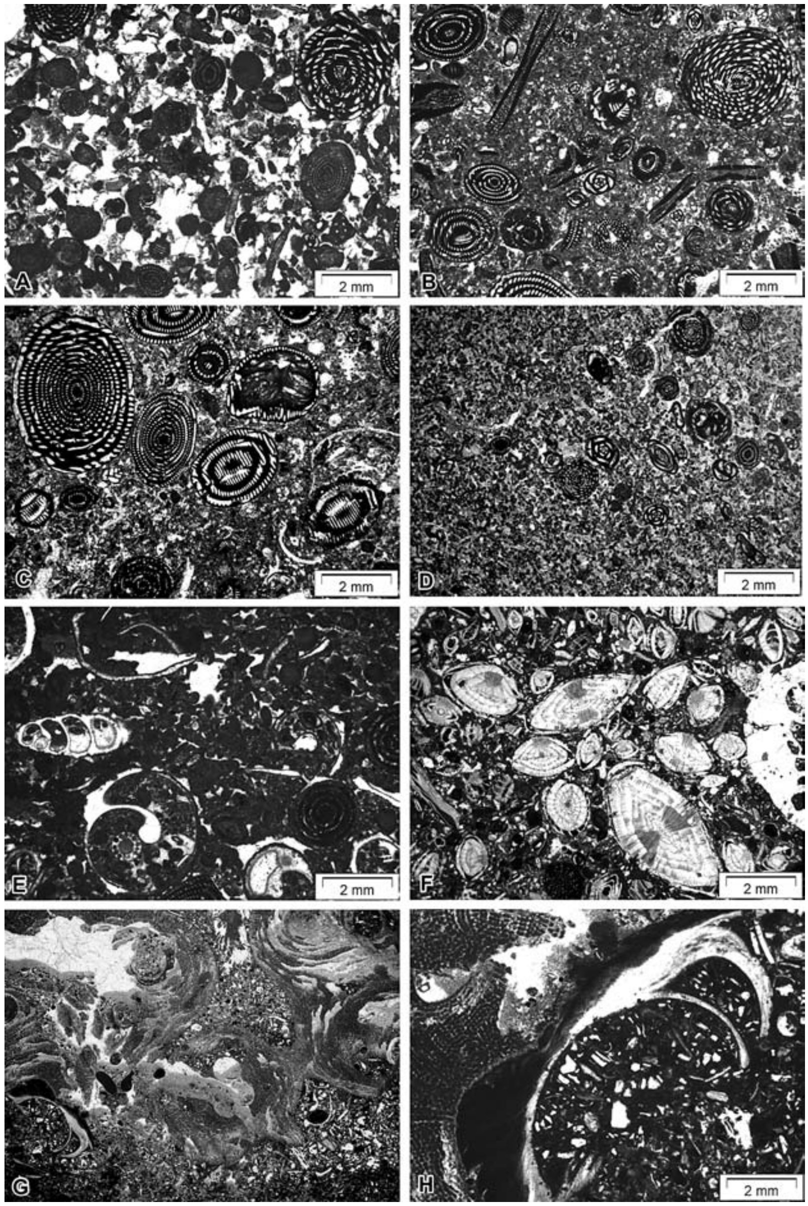

Fig. 4 Microfacies types from Minerve section, thin section images. **A** Terrigenous Alveolinid Facies, inner lagoon, sample M2-002. **B** Alveolinid–*Orbitolites* Facies, inner lagoon, sample M2-024. **C** Alveolinid Facies, outer lagoon, sample M2-023. **D** Bioclast Facies, bioclastic shoal, sample M2-029. **E** Gastropod-rich portion of Bioclast Facies, sample M2-033. **F** Nummulitid Facies, upper part of the middle ramp, sample M2-058. **G** Coral Facies, close to fair-weather wave base (image width: 45 mm), sample M2-052a. **H** Detail of (G) showing coral (left) growing over bivalve shell

lowest part, giving way to a pure carbonate succession upsection, mainly composed of alveolinid limestones. Nummulitids become more abundant upsection. According to Hottinger (1960), this section represents Early Ilerdian (SBZ 5 and 6). The semi-quantitative data are given in Appendix 1. The following microfacies types can be distinguished on the basis of field and microscopic investigations (Fig. 4):

Terrigenous Alveolinid Facies

Terrigenous alveolinid packstones, dominated by alveolinids (up to 40% of components) with up to 10% arenitic siliciclastics. Bioclasts (i.e., fragmented, mostly unidentified skeletal grains) contribute up to 30%. Subordinate components are peloids (i.e., micritized, rounded, arenitic components of unknown origin), miliolid smaller foraminifera, unidentified rotaliids, as well as scarce orbitolitids, and agglutinated smaller foraminifera. Alveolinids comprise a high degree of fragmentation and pressure solution. Distinct cross-bedding can be recognized in the field, but is not evident from thin sections. Wave ripples are also visible in the field; they are restricted to this facies. This facies is restricted to basal portions of the Minerve section. It is particularly different from other types by dominance of alveolinids accompanied by a relatively high content of arenitic siliciclastics.

Interpretation: Siliciclastics suggest a position close to a source area, i.e., close to the shoreline, which is supported by a high degree of fragmentation of bioclasts and its restriction to the very base of the carbonate succession. This is also reflected by the occurrence of cross-bedding, which is subordinate in other facies types, and wave ripples.

Alveolinid–Orbitolites facies

Alveolinid–orbitolitid packstones and pack/grainstones: Main components are alveolinids (up to 40%) as well as *Orbitolites* and bioclasts (both of them attributing 10–30% of the components). Peloids can be abundant as well (5–25%). Subordinate components are miliolid smaller foraminifera, few agglutinated smaller foraminifera, and rotaliids. A few samples contain sporadic dasycladalean algae, coralline algae, nummulitids, mollusc fragments, and siliciclastics. Fragmentation is low to absent in samples comprising pure packstones. This facies reveals the highest abundance of orbitolitids in the studied material.

Interpretation: The presence of orbitolitids suggests a protected shallow-water environment (Hottinger 1983; Gietl 1998). This is supported by the high abundance of alveolinids and the dominance of a micritic groundmass. Its lateral paleoenvironmental relationship with the Alveolinid Facies is shown by the fact that it is over- and underlain by the Alveolinid Facies in most cases.

Alveolinid Facies

Alveolinid packstones, a few grainstones, but mostly pack/grainstones: Alveolinids dominate (30 to >50%), followed by bioclasts (15–30%), peloids (mostly 15%), and smaller miliolid foraminifera (5–10%). All other components account for less than 5% each, with orbitolitids and agglutinated smaller foraminifera being most frequent; coralline algae are absent. Fragmentation of larger foraminifera is rare. This facies is the most abundant one, especially in lower parts of the section. Cross-bedding is visible in the field; it is most abundant in this facies.

Interpretation: Alveolinids are main components in Early and Middle Eocene shallow-water carbonates. They were most prominent in protected shelf and higher-energetic shoal environments (e.g., Hottinger 1983) and occurred in relatively deeper (or more offshore) waters than orbitolitids.

Alveolinid–Bioclast Facies

Alveolinid–bioclast pack/grainstones and grainstones: Alveolinids, bioclasts, and peloids display equal mean abundances (10–30%), followed by miliolid smaller foraminifera (up to 10%). All other components are subordinate and distributed irregularly among the samples. This facies does not form thick successions, but is distributed all over the section.

Interpretation: This facies represents a higher-energetic environment than the Alveolinid Facies. This is reflected by a lower abundance of micrite and the high abundance of rounded bioclasts. Both with respect to composition and environment, it reveals a transitional facies between the Alveolinid Facies and the Bioclast Facies. This is also proven by the fact that it is over- and underlain only by these two facies types.

Bioclast Facies

Mostly bioclastic pack/grainstones and grainstones, with subordinate pure packstones. Bioclasts (up to 50%) and peloids (10–20%) are the most abundant components. Miliolid smaller foraminifera account for 5–20%, while alveolinids and other components are mostly subordinate. This facies is most prominent in higher parts of the Minerve section.

Interpretation: Due to the dominance of bioclasts and the low abundance of micrite, this facies reflects the highest energetic environment of the studied material, and probably formed a bioclastic shoal.

Alveolinid–Nummulitid Facies

Alveolinid–nummulitid pack/grainstones and packstones: This facies reveals an equal abundance of alveolinids and nummulitids (10–30%). Also bioclasts, peloids, and miliolid smaller foraminifera are abundant. This facies occurs in higher parts of the section.

Interpretation: Since alveolinids and nummulitids thrive in different environments (e.g., Hohenegger et al. 1999), this facies reflects an offshore-transport of alveolinids into the Nummulitid Facies. Alveolinids obviously derive from environments of the Alveolinid–Bioclast Facies and Bioclast Facies, which represent the prominent over- and underlying facies types.

Nummulitid Facies

Nummulitid packstones. The name-giving foraminifera account for up to 50% of the components. Bioclasts can be abundant, other components, such as miliolid smaller foraminifera and corals, are subordinate. The degree of fragmentation is relatively high and microboring of nummulitids is abundant.

Interpretation: As already figured out by Hottinger (1983), nummulitids represent the relatively deepest organisms among the observed components. The combination of micritic matrix and relatively high degree of fragmentation points to textural inversion (Folk 1962) that can be explained by a low-energetic environment that was subjected to occasional high-impact storms. They were strong enough to cause fragmentation, but did not last long enough to wash-out the micritic groundmass. This suggests that the Nummulitid Facies was deposited below fair-weather wave base.

Bivalve facies

Bivalve rudstones and floatstones with different types of matrices: bioclast pack/grainstones, alveolinid–bioclast pack/grainstones and packstones, alveolinid–nummulitid packstones, and nummulitid packstones. This facies occurs in the middle parts of Minerve section.

Interpretation: Considering the dominance of packstone and pack/grainstone matrices as well as due to the matrix-forming biota (see interpretations above), this facies formed below and around the fair-weather wave base.

Coral facies

Coral rudstones with bioclastic packstone matrix revealing reworked coral heads. They are restricted to one sample.

Interpretation: Due to the bioclastic matrix and the reworked character of corals, accompanied by the prevalence of packstones, this facies was developed among relatively quiet-water conditions of the bioclastic shoal.

Campo section

The Paleocene facies types of Campo are completely different from those of the Eocene (Fig. 5). A particular Paleocene element is *Distichoplax biserialis*, a taxonomically uncertain calcareous red alga that is generally restricted to this time interval. It occurs in rock-forming quantities (*D. biserialis* grainstone in Fig. 5) or together with coralline red algae as well as corals (coral algal (*D. biserialis*) boundstone). Rhodoliths, which can occur together with corals and bryozoans (rhodolith boundstone and coral algal rhodolith boundstone with bryozoans), are also characteristic for the Paleocene of Campo section. The Ilerdian facies types described below were deposited above the karstified horizon with *Microcodium* sp. (see above).

This chapter summarizes the carbonate facies of the Early Ilerdian (SBZ 5 and SBZ 6) and compares them with Minerve. Since Campo only represents a reference section for the current study, facies types are studied in lesser detail than for Minerve. In order to avoid confusion with detailed facies types of Minerve, we only use rock-nomenclature terms (summarized by Flügel 2004).

Alveolinid packstones

The alveolinid packstones of the Campo section includes the Alveolinid–*Orbitolites* Facies, the Alveolinid Facies, and the Alveolinid–Bioclast Facies of Minerve (see above).

Miliolid wackestone

This type is dominated by smaller miliolids. Alveolinids, orbitolitids and agglutinated foraminifera with subordinate peloids, corals and echinoderms are present. This facies type is somewhat comparable to the Alveolinid–Bioclast Facies of Minerve, but the dominance of smaller miliolids hint to more restricted environments.

Restricted facies

This facies type is very heterogeneous. The first subtype is a bind- to wackestones with laminated algal structures and smaller miliolids. A second subtype is composed of ostracods and small benthic foraminifera in a micritic groundmass. The third subtype is dominated by large bivalves, and the fourth subtype by arenitic quartz grains in a micritic groundmass. The four subtypes of the restricted facies are by a low diverse fauna within a micritic groundmass. The laminated algal structures in combination with miliolids, ostracods and quartz grains are typical for restricted inner lagoonal environments. Its paleoenvironment is in a more onshore position than the larger foraminifera facies types.

Coral wacke-boundstone

Coral boundstone to wackestones with abundant coralline algae. Additional components are echinoderms and small miliolids. Larger foraminifera are not present. This facies type is present in only one interval.

Nummulitid wackestones

The components are dominated by nummulitids, predominantly *Assilina* sp. and subordinate *Nummulites* sp. that are often fragmented. Additional components are echinoderms, *Discocyclina* sp. smaller miliolids and bryozoans. Alveolinids are very rare and orbitolitids are absent. The upper part of the section is made up of this facies type. The presence of the nummulitids and the scarcity of alveolinids and orbitolitids in a micritic matrix indicate deposition well below the fair-weather wave base. With the deposition of this facies type the increased subsidence in the Campo section started (Eichenseer and Luterbacher 1992). It is comparable with the Nummulitid Facies in Minerve.

Serraduy section

In contrast to the Campo section, where the Paleocene is completely marine, the Serraduy section (Fig. 6) is dominated by terrestrial marls with minor marine horizons that are comparable to the coral–foraminiferal–algal facies types in the Paleocene of Campo. According to Eichenseer and Luterbacher (1992) and Robador et al. (1991), the Paleocene–Eocene boundary is situated within a 10 m interval above the massive conglomerates (110 m in Fig. 6) and the first alveolinid limestones (120 m). This chapter summarizes the main facies types of the Early Ilerdian and compares them with Minerve. Like for Campo, we only use rock-nomenclature.

Fig. 5 Geological column of the studied parts of the Minerve section and distribution of main facies types (stratigraphy after Orue-Etxebarria et al. 2001)

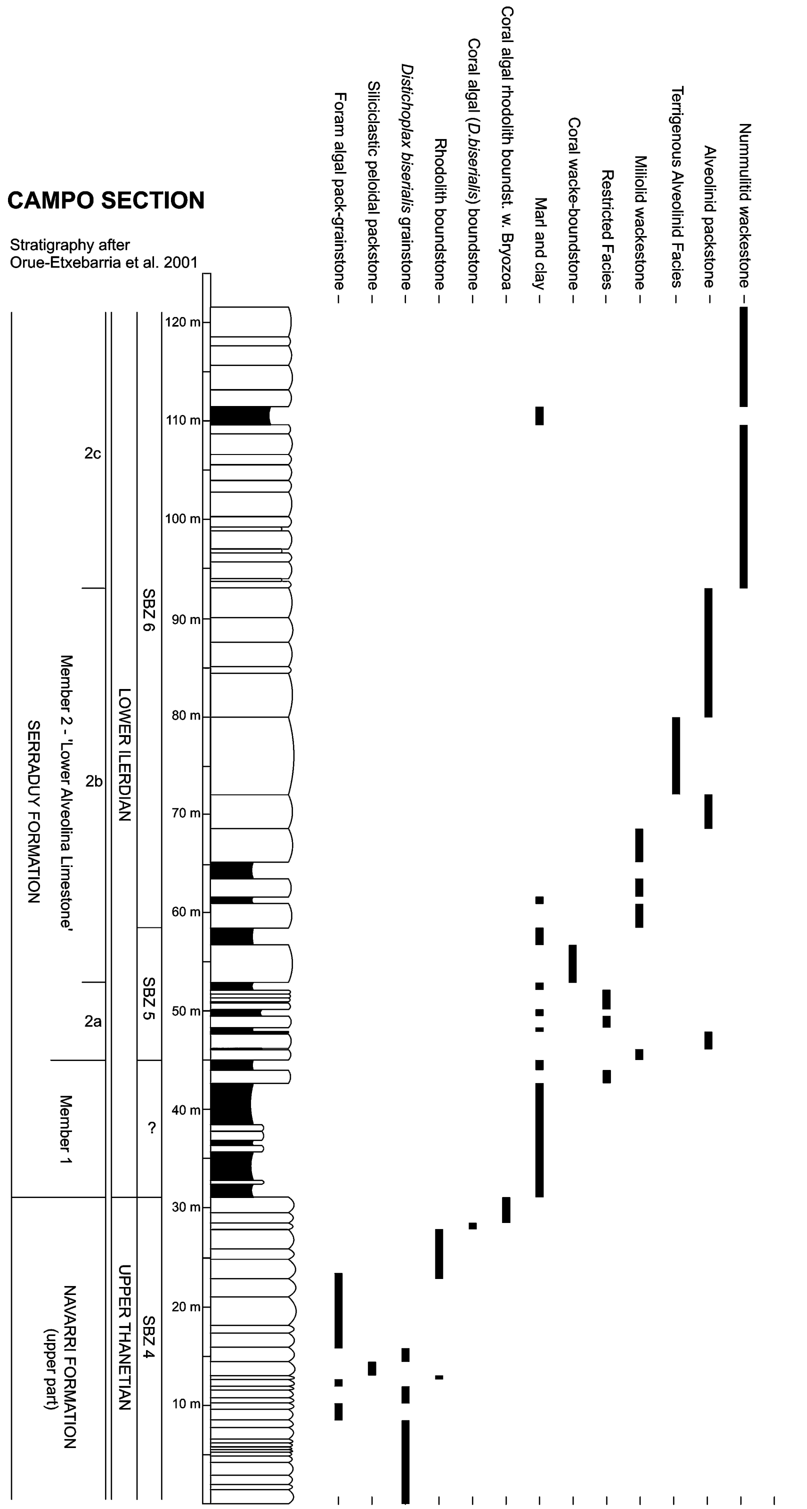

Coral wacke-boundstone

It is similar to the coral wacke-boundstone of Campo. Additionally, the encrusting foraminifera *Acervulina* sp. can be present.

Peloid grainstone

Peloids are the dominant components; subordinate miliolids, gastropods, rotaliids, dasycladaleans and arenitic quartz grains are present. The absence of micrite shows the influence of wave agitation and points to the highest energy index of the presented microfacies types. This facies probably accumulated in shoals close to the sea level.

Gastropod wackestone

This facies is dominated by gastropods and shell fragments in a micritic groundmass. Additionally, dasycladaleans, alveolinids, orbitolitids, and smaller miliolids are present. The association of the biogenic components suggests deposition in a more restricted environment with a more onshore position than the larger foraminiferal microfacies types.

Alveolinid packstone

The alveolinid packstone of the Campo section is comparable with the Alveolinid–*Orbitolites* Facies, the Alveolinid Facies, and the Alveolinid–Bioclast Facies of Minerve.

Siliciclastic bioclastic packstone

The bioclastic packstone is by abundant small quartz grains. Besides quartz, alveolinids, orbitolitids, miliolids, dasycladaceans, corals, shell fragments, and gastropods are present.

Discussion

Paleoenvironmental evidence from larger foraminifera

The most prominent components of the studied sediments are larger foraminifera: alveolinids, nummulitids and orbitolitids. The Paleogene was a time of particular abundance and radiation of these miliolid and hyaline larger foraminifera and especially during the Eocene they occur in rock-forming quantities. Due to their well-defined paleecological requirements, they represent valuable facies indicators. This chapter summarizes relevant key aspects from the review of Hohenegger (1999) about present-day larger foraminifera and their implications for fossil equivalents.

Like zooxanthellate corals, many larger foraminifera host symbiontic microalgae. The host uses photosynthates of the microalgae as an energy source for metabolic processes and can digest the symbionts in case of starvation or increasing density. Symbionts, on the other side, are protected within the foraminiferal test and are provided with carbon dioxide formed during secretion of the foraminifers carbonate test. In some cases, the host-symbiont system becomes completely photo-autotrophic, i.e., the foraminifers become independent from additional food uptake. This system allows larger foraminifera to settle under oligotrophic conditions in shallow tropical environments. In fact, larger foraminifera reach their maximum abundances and sizes under warm-water conditions, such as *Nummulites* with test diameters of up to 16 cm (Ungaro 1994). Hohenegger

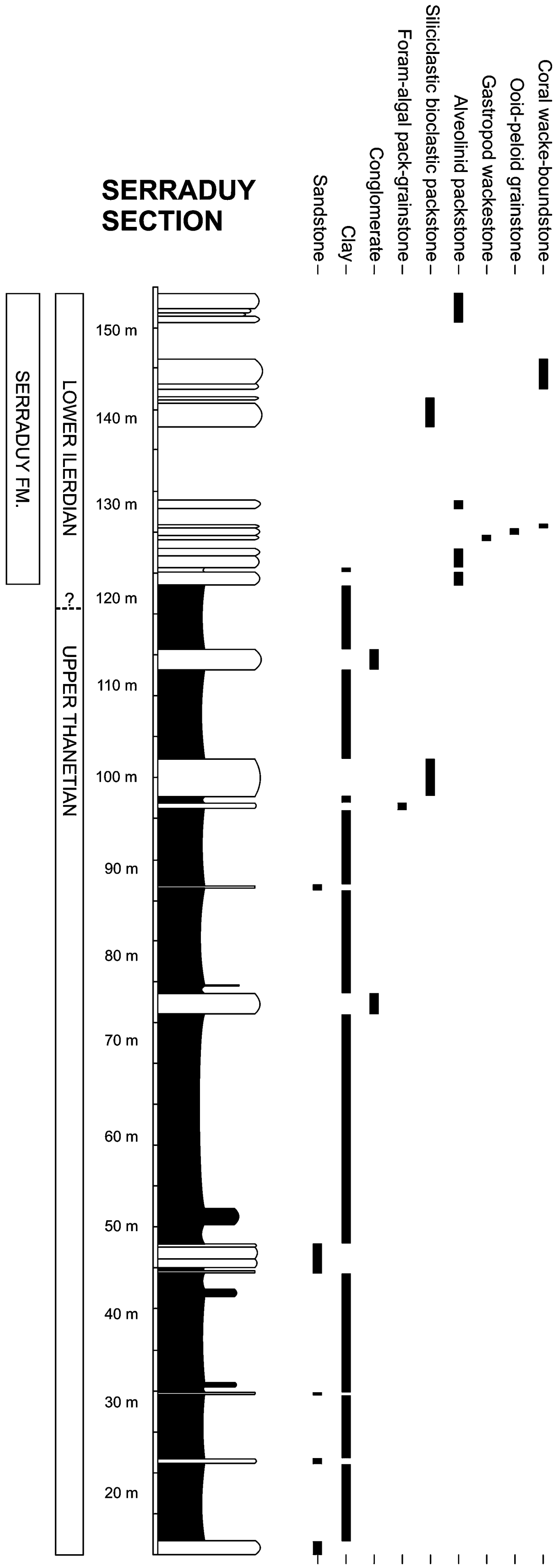

Fig. 6 Geological column of the Serraduy section

(1999) argues that these large diameters are caused by an intensive carbonate secretion during the whole life span necessary for promoting symbionts with sufficient carbon dioxide.

Fossil nummulitids, alveolinids, and orbitolitids are supposed to bear photo-symbiontic micro-algae, which explains their maximum abundances in oligotrophic, tropical shallow-marine environments. To a high degree the local distribution patterns of these three taxa in tropical environments can be explained by light intensity. As summarized above, symbiont-bearing foraminifera depend on light. However, they also need to protect themselves from very high degrees of illumination causing damage by ultra-violet light. This protection is brought about by non-transparent wall structures among miliolids (alveolinids, orbitolitids), which are therefore able to thrive in extremely shallow (i.e., highly illuminated) water. Nummulitids are, however, characterized by transparent, hyaline walls and therefore protect themselves from UV-light by producing very thick, lamellated test walls, or they occur in relatively deeper water.

Hydrodynamic energy, or mobile substrate, respectively, is another factor controlling the distribution of these three foraminifer groups and is expressed by their test morphologies. Two different test shapes reflect adaptation to high hydrodynamic energy: (1) thick lenticular tests, such as some nummulitids, or (2) rigid fusiform tests with lots of secondary chamberlet walls, such as alveolinids. Large, flat tests (e.g., orbitolitids and some nummulitids) are generally inappropriate for high-energetic settings because even normal wave agitation can cause floating. Nevertheless, such forms can occur in present-day shallow-water environments because they occur in protected areas, or they are attached to seagrass or macroalgae (e.g., Soritidae); a comparable life habit may be assumed for *Orbitolites*.

Considering comparable actuopaleontological approaches, the following distribution of the mentioned foraminifera has been established for Early Eocene carbonate environments (e.g., Ghose 1977; Hottinger 1983; Pautal 1987). From shallower to deeper water, the following generalized trend of larger foraminifera distribution can be distinguished: (1) discoidal miliolid forms, such as *Orbitolites* in protected, inner parts; (2) fusiform miliolid forms, such as *Alveolina*, in shallow, partly high-energetic areas; (3) thick lenticular hyaline forms, such as lenticular *Nummulites*; and finally (4) flat lenticular or discoidal hyaline forms, such as orthophragminids and flat species of *Nummulites* and *Assilina*. This deepening-upward trend provides a main base for our further interpretations given below.

Carbonate shelf geometries

The paleogeographical situation (Fig. 2) shows that the studied carbonate systems formed carbonate platforms attached to a continental hinterland. Consequently, two platform geometries can be considered, namely rimmed shelfs (e.g., Wilson and Jordan 1983) and carbonate ramps (e.g., Burchette and Wright 1992; reviewed in Flügel 2004). Pujalte et al. (1993) suggested a distally steepened ramp geometry for the northern Iberian margin. The absence of a rimmed shelf is clearly evident from the geological situation, since ramp structures, partly resembling mixed carbonate–siliciclastic ramps (Thanetian of Campo, Thanetian and Ilerdian of Serraduy), are most typical for foreland basins (e.g., Dorobek 1995). Furthermore, reefal bodies that might have formed a structural rim could not be recognized in the current study. Corals found in the studied material may have formed biostromes, but not frameworks with a particular structural relief growing up to the sea level.

Whether carbonate ramps were distally steepened (as suggested by Pujalte et al. 1993) or homoclinal, cannot be confirmed by the current study, since we are focusing on the shallowest environments. According to Burchette and Wright (1992), carbonate ramp environments are separated into (1) the inner ramp between upper shoreface and fair-weather wave base, which is constantly affected by wave agitation, (2) the middle ramp, between fair-weather wave base and storm-wave base with sediment reworking by storms (water depths between a few tens of metres and 100–200 m), and (3) the outer ramp below normal storm-wave base down to the basin plain.

As a result of the facies interpretations and palecology of larger foraminifera given above, it can be stated that inner ramp and higher portions of the middle ramp environments are present among the studied material: Inner ramp settings are characterized by alveolinid-dominated facies types, partly with *Orbitolites*, whereby the latter settled the inner-most, more protected parts; middle ramp settings are dominated by nummulitids as well as local bivalve- and coral-rich facies types (Fig. 7).

Carbonate factories

Carbonate factories are generally defined as subtidal areas comprising high carbonate production by predominantly benthic organisms (Schlager 2000; Flügel 2004). The term carbonate factory includes not only the space where carbonate is produced, but also the processes that lead to carbonate production (Schlager 2003).

Schlager (2000) defined three benthic carbonate factories: tropical, cool-water, and mud-mound factories. Modes of autochthonous marine carbonate production in these factories are abiotic precipitation (e.g., ooids), biotically induced precipitation (e.g., cyanobacterial mats), and biotically controlled precipitation (especially skeletal). The latter can be formed by photo-autotrophic or heterotrophic organisms. Both the carbonate factory types, and the modes of precipitation represent particular end-members of complicated processes and can show transitions between each other. For example, tropical factories can change into cool-water factories, if upwelling occurs, and carbonate cementation can be influenced by metabolic processes. Carbonate factories were recently reviewed by Schlager (2003).

The studied Early Ilerdian carbonate systems comprise the typical end-member of a tropical factory. The major precipitation mode is a biotically controlled one, with larger

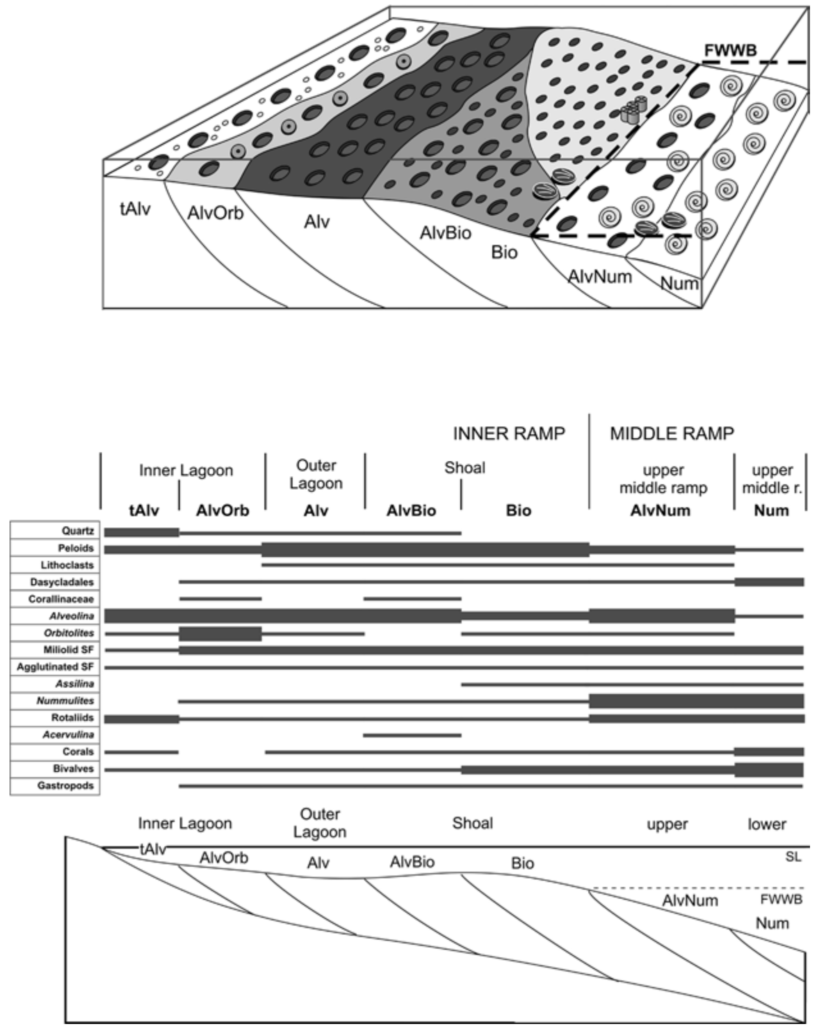

Fig. 7 Paleoenvironmental model for the tropical carbonate factory of an Ilerdian carbonate ramp, based on Minerve section (above; compare with Fig. 3) and distribution of main components along the ramp profile. Inner and outer ramp environments are separated by the fair-weather wave base. Facies types: tAlv: Terrigenous Alveolinid Facies; AlvOrb: Alveolinid–*Orbitolites* Facies; Alv: Alveolinid Facies; AlvBio: Alveolinid–Bioclast Facies; Bio: Bioclast Facies; AlvNum: Alveolinid–Nummulitid Facies; Num: Nummulitid Facies. Other abbreviations: FWWB: fair-weather wave base; SF: smaller foraminifera; SL: mean sea level

foraminifera being the main agents as well as scarce corals. Due to the live mode of alveolinids and nummulitids, they represent photo-autotrophic agents. Heterotrophic organisms, i.e., bivalves, gastropods, bryozoans, and vermetids, are subordinate. Biotically induced precipitates are also abundant; they are represented by micritic envelopes of bioclasts as well as most of the peloids, which we interpret to originate from micritized bioclasts. Abiotic carbonate precipitation is particularly scarce and restricted to ooids from parts of the Campo section. It could also be represented by submarine carbonate cement precipitation within foraminiferal chambers, but we did not find reliable evidence for this.

The tropical factories operate in warm, oligotrophic, highly illuminated, oxygenated waters (i.e., today's tropical belt). Therefore, the depth window of carbonate production in tropical factories is shallower and much narrower than in other factories: the average production rate is highest from the intertidal range down to ca. 30 m, with a strong decline down to a depth of ca. 50 m, followed by a reduction to zero around 100 m (Schlager 2003). Consequently, the highest rate of carbonate production should occur in inner ramp and higher middle ramp settings described in this paper.

Influence of the Paleocene–Eocene Thermal Maximum

The Early Paleogene is characterized by a long-term rise of global sea-surface temperatures and CO_2 values (Zachos et al. 2003), resulting in conditions unfavorable for corals and coralline algae. As discussed by Scheibner et al. (in press), photo-symbiontic larger foraminifera are affected by these conditions to a lesser degree. Within this interval of global temperature rise, eutrophic conditions caused by the Paleocene–Eocene Thermal Maximum (PETM) are expected to represent only a short-term perturbation of a long lasting oligotrophic trend (Scheibner et al. in press). In the studied sections, this trend of increased temperatures may be expressed by the minor importance of hermatypic corals and coralline algae in the Early Ilerdian, when compared to the Late Paleocene. Consequently, the studied Early Ilerdian facies types represent a post-PETM return to oligotrophic conditions, while the studied latest Paleocene algae-dominated facies types may reflect more eutrophic conditions in the course of the PETM. Therefore, the Early Ilerdian facies types express an important stage in the Early Paleogene climatic development and evolution of nummulitids and alveolinids (Larger Foraminifer Turnover: Hottinger 1998; Orue-Etxebarria et al. 2001).

Although the described dominance of algae and the occasional abundance of bryozoans during the latest Paleocene of Campo section point to more eutrophic environmental conditions, it is interesting to note that the type of carbonate factory (Schlager 2003) is largely the same as in the Early Ilerdian: A tropical carbonate factory (as suggested by the high abundance of hermatypic corals) with a dominance of biotically controlled precipitation by photo-autotrophic organisms (corals, red algae).

Synthesis: paleoenvironmental model of an Early Ilerdian, tropical carbonate factory

This chapter provides a synthesis as a basis for a detailed standard shelf profile for Early Ilerdian carbonate factories as shown in Fig. 7. It is based on a detailed microfacies and field analysis of the Minerve section combined with additional data from Campo and Serraduy.

Paleoenvironmental model

For the inner carbonate ramp environments, three subenvironments can be distinguished, herein named inner lagoon, outer lagoon, and shoal. Inner lagoonal environments are dominated by alveolinid foraminifera. In basal parts of the section they can show cross-bedding and terrigenous influence from the hinterland. The highest abundance of orbitolitid foraminifera occurs in this area. They reflect either hydrodynamical-protected areas, or the existence of meadows formed by seagrass or fleshy macroalgae. The outer lagoon is also dominated by alveolinid foraminifera, but siliciclasts are absent and orbitolitids are less abundant. Micrite is less abundant than in the inner lagoon, but still dominates the groundmass.

The shoal area is characterized by a high abundance of rounded bioclasts. It reveals two different facies types: the Bioclast Facies and the Alveolinid–Bioclast Facies. The latter represents a transition between the two end-members Alveolinid Facies (outer lagoon) and Bioclast Facies (highest-energetic part of the shoal). High-energetic and structurally complex nummulite shoals are absent. Instead, the facies successions and microfacies criteria suggest that nummulitids were most abundant in the middle ramp settings (see below). This could be due to the lower abundance and size of these foraminifera during the Early Ilerdian, whereas nummulite shoals are more characteristic for the Middle Eocene (e.g., Aigner 1983; Serra-Kiel and Reguant 1984; Ungaro 1994).

Close to the fair-weather wave base, patches with bivalves thrived, forming a secondary substrate enabling the growth of hermatypic corals, which may have formed coral carpets. The restriction of corals to this secondary substrate and the absence of rigid coral frameworks are evidence for the high mobility of the substrate and repeated storm events reworking the sediment.

The middle ramp settings, below normal wave agitation but affected by occasional storms, are characterized by the highest abundance of nummulitids and diverse other rotaliids. The Nummulitid Facies forms the deepest part of the studied sediments. Also bivalves are most abundant in this environment. The Alveolinid–Nummulitid Facies comprises a transitional facies between the deeper Nummulitid Facies and the shallower Alveolinid or/and Alveolinid–Bioclast Facies. There, alveolinids are swept from the inner platform down to the middle ramp, where nummulitids lived.

The carbonate factory

The studied sediments developed in oligotrophic, tropical, normal-marine, well-oxygenated, mostly well-agitated, shallow waters of the upper photic zone. They represent the end-member of a tropical carbonate factory, dominated by biotically controlled carbonate preciptiation by photo-autotrophic organisms and—to a lesser degree—by biotically induced micritization. Also the precipitation modes represent end-members. Given these environmental characters, one would expect a high degree of (abiotic) submarine carbonate cement precipitation. We found, however, no evidence for early marine cementation.

All studied carbonate environments represent areas of main carbonate production. The main agents of photo-autotrophic, biotically controlled carbonate precipitation are alveolinids in inner and outer lagoonal settings as well as nummulitids in middle ramp settings. Patchy heterotrophic counterparts are represented by bivalve accumulations around fair-weather wave base. The main agent of biotically induced carbonate precipitation is micritization in outer lagoonal and especially in shoal environments. A type of carbonate export can be recognized in the down-ramp transport of alveolinid tests, i.e., from the inner ramp setting into upper parts of nummulitid-dominated middle ramp environments.

Acknowledgements This study was supported by the German Science Foundation (DFG) project "Linking biocalcification to the global carbon cycle: carbonate systems during the Paleogene", DFG MU 1680/5-1. We wish to thank A. Freiwald (Erlangen) for a thorough review, H. Weissert (Zürich) for stimulating discussions, Y. Tambareau and F. Christophoul for an introduction to the Paleocene–Eocene sections in SW France, and Christine Fischer (Potsdam) for preparation of thin sections.

Appendix 1: Semiquantitative distribution of components of Minerve

Taba

Meters	Sample	Quartz	Peloids	Bioclasts	Lithoclasts	Dasycladales	Coralline algae	Alveolinids	Orbitolithids	Miliolid smaller foram	Agglutinated smaller foram	Assilina	Nummulites	Rotaliid foram	Acervulina	Plankton	Corals	Bryozoans	Vermitids	Bivalves	Gastropods
0.2	M2-001	2	1	3				5						1							
0.6	M2-002	2	1	3				4		1				1							
0.9	M2-003	2	1	2				4		1				1						1	
1.10	M2-004	1	1	3				4		1				1		1					
1.30	M2-005	3	1	3				4	1	1				1							
1.90	M2-006	2	2	3				4		1				1							
2.10	M2-007	2	2	3				3	1	1				1							
3.00	M2-008	1	1	3				3	1	1	1			1			2				
3.70	M2-009	3	2	3				2		2				1							
4.30	M2-010	2	2	3				4	1	1				1							
5.30	M2-011	1	2	2				3	1	1				1							
5.50	M2-012b		1	3				3	2	1											
6.20	M2-013		2	2		1		3	1	1				1		1					
6.60	M2-014		2	3				3	1	1	1			1						1	
7.4	M2-015		2	3	1	1		3		1				1		1					
7.9	M2-016		2	3	1			3	1	1	1			1							1
8.2	M2-017		2	3	1			3	1	1	1			1		1			1	1	
8.9	M2-018		2	2				4		1				1				1			
9.80	M2-019		1	3				5		1				1						1	1
11.00	M2-020		2	3				4		1				1			1		1		2
11.30	M2-021		1	3		1		5		1				1							1
11.60	M2-022		2	3				3		1	1			1							
12.00	M2-023		1	3		1		3		1	1			1							
12.30	M2-024		1	3				4	2	1	1			1							
12.70	M2-025		1	3				4	2	2	1			1							
13.10	M2-026		3	2		1		5		1	1			1							1
13.60	M2-027		3	2		1		5	1	2	1			1					1	1	1
14.10	M2-028		3	4				1		2	1					1					
14.30	M2-029		3	4				1		2	1										
14.70	M2-030	2	1	2				3		2				1							
15.00	M2-031	1	3	3				4		1	1			1					1	1	
15.40	M2-032		2	3				3		1				1							
15.70	M2-033		3	2		2		2		1				1					1	2	3
16.80	M2-035		2	2				2	1	1				1			5				1
17.20	M2-036		2	2				4	1	1	1		1	1							
17.60	M2-037		2	3				5	1	1	1		1	1							
18.00	M2-038		2	3				3	1	2			1	1						1	2
18.30	M2-039		2	3				3		1			1	1							1
18.70	M2-040		2	3				3		1			1	1							
19.50	M2-041		2	3				3	1	2	1			1		1					
20.40	M2-042		2	2	1			2	1	2				1							
20.90	M2-043a		2	2				4	2	2	1		1	2							
21.20	M2-044		2	3				3	1	2			1	2							1
21.60	M2-045		3	2	1			3		2			1	2							
21.90	M2-046a		2	2				4	1	2	1			1					1		
22.80	M2-047		2	2				4		1			1	1							
23.60	M2-048b		2	3				4	1	1	1			1						1	
24.10	M2-049		3	2		1		4	1	1	1			1							
25.90	M2-051		3	3				1	1	1	1		1	1					1	2	
26.25	M2-052		2	3				1		1							4			3	
26.60	M2-057			2		1				1			4	2						3	
27.00	M2-058			2		1				2	1		5	2			3			1	1
27.50	M2-060		3	2				1	1	1			2	1						2	1
27.80	M2-061		3	2				1	1	1			1	1			1			2	2

Taba Continued

Meters	Sample	Quartz	Peloids	Bioclasts	Lithoclasts	Dasycladales	Coralline algae	Alveolinids	Orbitolithids	Miliolid smaller foram	Agglutinated smaller foram	Assilina	Nummulites	Rotaliid foram	Acervulina	Plankton	Corals	Bryozoans	Vermitids	Bivalves	Gastropods
28.20	M2-062		2	3	1	1		2	1	1			1	1						1	
28.50	M2-063		2	2			1	3	3				1	1						1	
29.30	M2-064		2	2		1		3	3	2	1		1								
29.80	M2-065		1	2				4	1	1	1									1	
30.70	M2-066		2	3			1	3	1	1	1										
31.20	M2-067		2	2		1		2	1	1			1	1						1	1
32.90	M2-069		3	2				2	1	2	1			1						1	1
33.20	M2-070		3	2		1		3	3	1	1			1							1
33.80	M2-071		3	2				3		1	1										
34.20	M2-072		3	3				2	2	1										1	1
34.70	M2-073	1	2	3		1		3	1	1				1						1	1
35.20	M2-074	1		2		1		1		1			1	1				1		3	
35.50	M2-075		1	3	1	1		1		1	1	1	2	2						2	
35.90	M2-076		2	3		1		1		1		2	1	1			1	1		2	
36.50	M2-077		2	3				2	1	1	1	1	1	1			1			2	
37.00	M2-078		3	2				2	1	1										2	
37.70	M2-079		2	3		1		2	1	1		1	1	1				1			
38.60	M2-080		2	2				2	1	2	1			1							
39.40	M2-081		3	2				1	1	2			1								
40.00	M2-082		2	3				1	1	2			1	1							
40.60	M2-083		2	3		1		1	1	3	1									1	
41.20	M2-084		3	3		1		1	1	3	1		1								
41.50	M2-085		3	3						1	1										
41.80	M2-086		2	3		1		1	1	2	1									1	1
42.60	M2-087		3	2		1		1	1	2											
43.00	M2-088		2	3		1		2	1	1											1
43.15	M2-089		3	3				1	1	2	1										
43.70	M2-090		2	2		1		1	2	1	1									1	
44.30	M2-091		3	2	1	1		1	1	2	1			1							
44.90	M2-092		3	2		1		2	1	1										1	
45.40	M2-093		3	3	1			1		1	1									2	
45.90	M2-094		3	2		1		2		2	1							1		2	1
46.50	M2-095		3	2	1	1		1		3	1							1		1	
47.10	M3-001		2	3		1		1		1			1	1			2	1		1	
47.80	M3-002			2				3		1	1		3	1				1		1	
48.10	M3-003		2	2				3		1			3	1				1		1	
48.65	M3-004		1	3		1		3		1			2	3			1	1		2	
49.15	M3-005		3	2		1		3		1			1	2	1						
49.30	M3-006	1	2	2		1		4	2	2	1			1					1	1	1
50.20	M3-007	1	2	2		1		2	1	3				1							1
50.70	M3-008	1	2	2				3	1	3				1						1	1
51.20	M3-009	1	2	2				2		3			1	1						1	
51.70	M3-010		2	2				3		3			3	1							
52.00	M3-011		2	3		1		3		3			3	2							
52.40	M3-012		2	2				3		3			3	1						1	
52.80	M3-013		3	2		1		4	1	2			1							1	

References

Aigner T (1983) Facies and origin of nummulitic buildups: an example from the Giza Pyramids Plateau (Middle Eocene, Egypt). N Jh Geol Paläont Abh 166:347–368

Burchette TP, Wright VP (1992) Carbonate ramp depositional systems. Sediment Geol 79:3–57

Dickens GR, Castillo MM, Walker JCG (1997) A blast of gas in the latest Paleocene; simulating first-order effects of massive dissociation of oceanic methane hydrate. Geology 25:259–262

Dorobek SL (1995) Synorogenic carbonate platforms and reefs in foreland basins: controls on stratigraphic evolution and platform/reef morphology. SEPM Spec Publ 52:127–147

Eichenseer H, Luterbacher H (1992) The marine Paleogene of the Tremp Region (NE Spain)—depositonal sequences, facies history, biostratigraphy and controlling factors. Facies 27:119–152

Flügel E (2004) Microfacies of carbonate rocks. Springer, Berlin Heidelberg New York, 976 pp

Folk RL (1962) Spectral subdivision of limestone types. In: Ham WE (ed) Classification of carbonate rocks. AAPG Memoir 1:62–84

Ghose BK (1977) Paleoecology of the Cenozoic reefal foraminifers and algae, a brief review. Palaeogeogr Palaeoclimatol Palaeoecol 22:231–256

Gietl R (1998) Biostratigraphie und Sedimentationsmuster einer nordostägyptischen Karbonatrampe unter Berücksichtigung der Alveolinen-Faunen. Ber Fachb Geowiss Univ Bremen 112: 135

Hohenegger J (1999) Larger foraminifera—microscopical greenhouses indicating shallow-water tropical and subtropical environments in the present and past. Occ Pap Kagoshima Univ Res Cent Pacif Isl 32:19–45

Hohenegger H, Yordanova E, Nakano Y, Tatzreiter F (1999) Habitats of larger foraminifera on the upper reef slope of Sesoko Island, Okinawa, Japan. Mar Micropal 26:109–168

Hottinger L (1960) Recherches sur les Alvéolines du Paléocène et de l'Eocène. Schweiz Palaeont Abh 75/76:1–243

Hottinger L (1983) Processes determining the distribution of larger foraminifera in space and time. Utrecht Micropal Bull 30:239–253

Hottinger L (1998) Shallow benthic foraminifera at the Paleocene–Eocene boundary. Strata Ser 1 9:61–64

Hottinger L, Schaub H (1960) Zur Stufeneinteilung des Paleocaens und des Eocaens. Eclogae Geol Helv 53:453–479

Kapellos C, Schaub H (1973) Zur Korrelation von Biozonierungen mit Grossforaminiferen und Nannoplankton im Paläogen der Pyrenäen. Eclogae Geol Helv 66:687–737

Kennett JP, Stott LD (1991) Abrupt deep-sea warming, palaeoceanographic changes and benthic extinctions at the end of the Palaeocene. Nature 353:225–229

Luterbacher H-P (1984) Paleoecology of foraminifera in the Paleogene of the Southern Pyrenees. Benthos'83, 2nd International Symposium on Benthic Foraminifera, Pau, pp 389–392

Miller KG, Fairbanks RG, Mountain GS (1987) Tertiary oxygen isotope synthesis, sea level history and continental margin erosion. Paleoceanography 2:1–19

Molina E, Angori E, Arenillas I, Brinkhuis H, Crouch EM, Luterbacher H, Monechi S, Schmitz B (2003) Correlation between the Paleocene/Eocene boundary and the Ilerdian at Campo, Spain. Rev Micropaléont 46:95–109

Norris RD, Roehl U (1999) Carbon cycling and chronology of climate warming during the Palaeocene/Eocene transition. Nature 401:775–778

Orue-Etxebarria X, Pujalte V, Bernaola G, Apellaniz E, Baceta JI, Payros A, Nunez-Betelu K, Serra-Kiel J, Tosquella J (2001) Did the Late Paleocene thermal maximum affect the evolution of larger foraminifers? Evidence from calcareous plankton of the Campo Section (Pyrenees, Spain). Mar Micropal 41:45–71

Pautal L (1987) Foraminiferal assemblages of some Early Eocene environments (bays) from the northern Corbieres, France. In: Hart MB (ed) Micropaleontology of carbonate environments. Ellis Horwood, Chichester, pp 74–81

Pujalte V, Robles S, Robador A, Baceta JI, Orue-Etxebarria X (1993) Shelf-to-basin Palaeocene palaeogeography and depositional: sequences, western Pyrenees, North Spain. Spec Publ Int Assoc Sediment 18:369–395

Pujalte V, Orue-Etxebarria X, Schmitz B, Tosquella J, Baceta JI, Payros A, Bernaola G, Caballero F, Apellaniz E (2003) Basal Ilerdian (earliest Eocene) turnover of larger foraminifera: age constraints based on calcareous plankton and $\delta^{13}C$ isotopic profiles from new southern Pyrenean sections (Spain). In: Wing SL, Gingerich PD, Schmitz B, Thomas E (eds) Causes and consequences of globally warm climates in the Early Paleogene, vol 369. Geol Soc Am Spec Pap, Oklahoma, pp 205–221

Robador A (1991) Early Paleogene stratigraphy. In: Barnolas A, Robador A, Serra-Kiel J, Caus E (eds) Introduction to the Early Paleogene of the South Pyrenean Basin. Field-trip guidebook. 1st Meet IGCP Proj 286, Jaca 1990. Inst Tecnol Geomin España, Barcelona, pp 41–87

Robador A, Samso JM, Serra-Kiel J, Tosquella J (1991) Field guide. In: Barnolas A, Robador A, Serra-Kiel J, Caus E (eds) Introduction to the Early Paleogene of the South Pyrenean Basin. Field-trip guidebook. 1st Meet IGCP Proj 286, Jaca 1990. Inst Tecnol Geomin España, Barcelona, pp 131–159

Roehl U, Bralower T, Norris RD, Wefer G (2000) New chronology for the late Paleocene thermal maximum and its environmental implications. Geology 28:927–930

Schaub H (1966) Über die Grossforaminiferen im Untereocaen von Campo (Ober-Aragonien). Eclogae Geol Helv 59:355–377

Schaub H (1969) L'Ilerdien - État actuel du problème. Mém Bur Rech Géol Min 69:259–266

Schaub H (1992) The Campo Section (NE Spain) a Tethyan parastratotype of the Cuisian. N Jb Geol Paläont Abh 186:63–70

Scheibner C, Speijer RP, Marzouk A (in press) Larger foraminiferal turnover during the Paleocene/Eocene thermal maximum and paleoclimatic control on the evolution of platform ecosystems. Geology

Schlager W (2000) Sedimentation rates and growth potential of tropical, cool-water and mud-mound carbonate factories. In: Insalaco E, Skelton P, Palmer TJ (eds) Carbonate platform systems: components and interactions, vol 178. Geol Soc London Spec Publ, London, pp 217–227

Schlager W (2003) Benthic carbonate factories of the Phanerozoic. Int J Earth Sci 92:445–464

Schmitz B, Pujalte V (2003) Sea-level, humidity, and land-erosion records across the initial Eocene thermal maximum from a continental-marine transect in northern Spain. Geology 31:689–692

Serra-Kiel J, Reguant S (1984) Paleoecological conditions and morphological variation in monospecific banks of *Nummulites*: an example. Benthos'83, 2nd International Symposium on Benthic Foraminifera, Pau, pp 557–563

Serra-Kiel J, Hottinger L, Caus E, Drobne K, Ferrandez C, Jauhri AK, Less G, Pavlovec R, Pignatti J, Samso JM, Schaub H, Sirel E, Strougo A, Tambareau Y, Tosquella J, Zakrevskaya E (1998) Larger foraminiferal biostratigraphy of the Tethyan Paleocene and Eocene. Bull Soc Géol France 169:281–299

Tambareau Y (1994) Paleocene/Eocene boundary in the platform deposits of he Northern Pyrenees. Bull Soc Belg Geol 103:293–299

Tambareau Y, Villatte J, Crochet B, Deramond J, Eichene P, Guerrero N, Canudo J, Gruas-Cavagnetto C, Hottinger L, Molina E, Tosquella J (1994) Introduction to the Early Paleogene of the North Pyrenean Basin—field trip guide book. Early Paleogene Benthos. 4th IGCP 286 Meet, Haute-Garonne, France, 39 pp

Ungaro S (1994) Nummulite morphological evolution. Boll Soc Paleont Ital Spec Vol 2:343–349

Wing SL, Gingerich PD, Schmitz B, Thomas E (2003) Causes and consequences of globally warm climates in the Early Paleogene. Geol Soc Am Spec Pap 369:1–614

Wilson JL, Jordan C (1983) Middle shelf environment. In: Scholle PA, Bebout DG, Moore CH (eds) Carbonate depositional environments. AAPG Memoir 33:297–343

Zachos J, Pagani M, Sloan L, Thomas E, Billups K (2001) Trends, rhythms, and aberrations in global climate 65 Ma to present. Science 292:686–693

Zachos JC, Wara MW, Bohaty S, Delaney ML, Petrizzo MR, Brill A, Bralower TJ, Premoli-Silva I (2003) A transient rise in tropical sea surface temperature during the Paleocene–Eocene thermal maximum. Science 302:1551–1554